Optically Tunable Delay Line in Silicon Microring Resonator Based on Thermal Nonlinear Effect

Fangfei Liu, *Student Member, IEEE*, Qiang Li, *Student Member, IEEE*, Ziyang Zhang, Min Qiu, *Member, IEEE*, and Yikai Su, *Senior Member, IEEE*

***Abstract*—We experimentally demonstrate optically tunable delay line in a silicon microring resonator with a 20-μm radius. The delay-tuning mechanism is based on the red shift of the resonance induced by thermal nonlinear effect. We investigate the delay performance of three modulation formats—non-return-to-zero (NRZ), return-to-zero (RZ), and differential phase-shift keying (DPSK) signals at different data rates. Tunable delay is achieved by controlling the power of the continuous-wave (CW) pump with very low tuning threshold, which could be used in microring-resonator-based slow-light structure.**

***Index Terms*—Buffer, microring resonator, silicon photonics, thermal nonlinear effect.**

I. Introduction

Optical buffering is a key technology in future all-optical packet-switched networks as well as optical interconnections in computer systems to avoid traffic contention [1], [2]. On-chip optical buffers based on nanowaveguide might show significant impact on future integrated photonic systems [3]. The recently developed silicon-on-insulator (SOI) structure has been proved to be an excellent platform for monolithic integration of photonic devices due to its high index contrast between the silicon core and the silica cladding, which allows strong confinement of light and enables ultracompact devices [4]. Some on-chip delay lines based on silicon waveguide have been demonstrated including the cascaded-microring-resonator-based all-pass filters (APFs) structure, coupled resonator optical waveguides structure [3], stimulated Raman scattering (SRS)-controlled slow-light delay line in silicon waveguide [5], as well as slow-light in silicon resonator enhanced by SRS [6]. Among these studies, only Xia *et al*. [3] have investigated the delay performance of real data packet, however, without delay tunability. Tunable delay line is a key element for implementing a practical buffer. For a microring-resonator-based delay line, there are mainly three types of methods to realize tunable group delay: 1) electrooptic effect by doping the intrinsic silicon to form a p-i-n structure [7]; 2) thermooptic effect by implanting a microheater in the microring resonator [8]; and 3) MEMS-actuated structure [9]. However, these methods need additional procedure in the fabrication process. As the absorption of a pump light would be eventually converted to the thermal energy [10], the injection of the pump light can also lead to thermal nonlinear effect and red-shift the resonance, which could be used to change the group delay of a probe signal by varying the intensity of the pump power. With a continuous-wave (CW) optical input, this thermal nonlinear effect can dominate over the carrier nonlinear effect with proper device size, and the effect possesses the lowest power requirement relative to other optical tuning mechanisms [10], [11]. In this paper, we experimentally investigate the delay performances of three widely used modulation formats in optical communications—nonreturn-to-zero (NRZ), return-to-zero (RZ), and differential phase-shift keying (DPSK) with pseudorandom bit sequence (PRBS) pattern at different data rates. These data pass through a 20-μm-radius single-side-coupled silicon microring resonator, which is controlled by a CW pump signal to induce thermal nonlinear effect.

In Section II, we introduce the device and the vertical coupling method to couple the light into the silicon nanowire; in Section III, we describe the principle of the thermal nonlinear effect induced by the absorption of the pump light and provide the experiment setup; in Section IV, we show the experimental results including the delayed waveforms and the dependence of the delay on the pump power for the three modulation formats at different data rates.

II. Device and Its Coupling to the Fiber

A. Silicon Microring Resonator

The 20-μm-radius silicon microring resonator in our experiment is fabricated on an SOI wafer with a 250-nm-thick silicon slab on top of a 3-μm silica buffer layer to prevent the optical mode from leaking to the substrate. The cross section of the silicon waveguide is 450×250 nm with a mode area of about 0.1 μm^2 for transverse-electric (TE) optical mode in such a high-index-contrast structure. The microring is side coupled to the straight waveguide with an air gap of 120 nm between the straight waveguide and the microring. The device is fabricated by E-beam lithography followed by reactive ion etching. The surface roughness is reduced by oxidizing 20 Å of silicon surfaces using wet chemistry. The scanning electron microscope

Manuscript received November 1, 2007; revised December 30, 2007. This work was supported in part by the NSFC under Grant 60777040, in part by the 863 High-Tech Program under Grant 2006AA01Z255, in part by the Shanghai Rising Star Program Phase II under Grant 07QH14008, and in part by the Fok Ying Tung Fund under Grant 101067. The work of Z. Zhang and M. Qiu was supported in part by the Swedish Foundation for Strategic Research (SSF) through the Future Research Leader Program and in part by the Swedish Research Council (VR).

F. Liu, Q. Li, and Y. Su are with the State Key Laboratory of Advanced Optical Communication Systems and Networks, Department of Electronic Engineering, Shanghai Jiao Tong University, Shanghai 200240, China (e-mail: yikaisu@sjtu.edu.cn).

Z. Zhang and M. Qiu are with the Department of Microelectronics and Applied Physics, Royal Institute of Technology (KTH), 164 40 Kista, Sweden.

Color versions of one or more of the figures in this paper are available online at http://ieeexplore.ieee.org.

Digital Object Identifier 10.1109/JSTQE.2008.916240

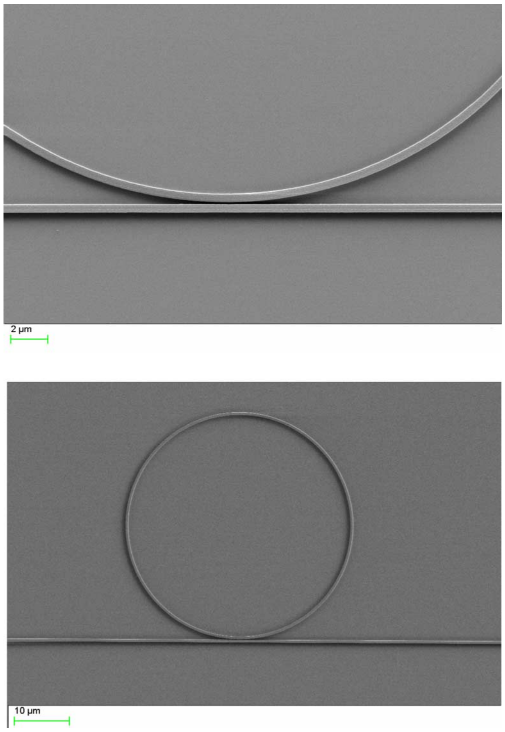

Fig. 1. SEM photographs of the silicon microring resonator with a radius of 20 μm.

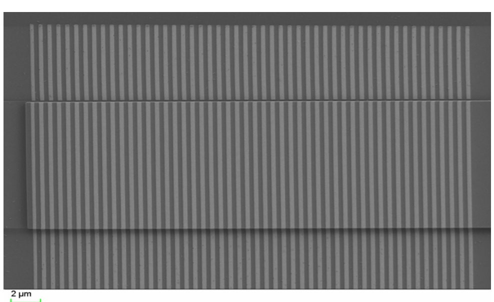

Fig. 2. SEM photographs of the gold grating coupler.

(SEM) photographs of the silicon microring resonator are shown in Fig. 1.

B. Vertical Coupling

At each end of the straight silicon waveguide, there is a gold grating coupler to couple the light between the single-mode fiber (SMF) and the silicon waveguide [12]. Fig. 2 shows the SEM photograph of the gold grating coupler at the end of the straight waveguide. The grating coupler is polarization dependent, and for a 600-nm period and a filling factor 45%, it only supports the TE mode. The input and output fibers should be placed under a certain angle (typically 10°) relative to the vertical axis upon the grating coupler. There is an adiabatic taper between the grating coupler and a 250-μm-long access straight waveguide. The gold grating coupler is wavelength sensitive and has a wavelength response curve with a 3 dB bandwidth of 30 nm at the 1550-nm telecommunication wavelength. This vertical coupling method has advantages in terms of easy alignment and simple fabrication of the mode converter compared to other coupling methods. The measured fiber-to-fiber coupling loss is ~20 dB.

III. OPERATING PRINCIPLE AND EXPERIMENT SETUP

A. Operating Principle

The linear transfer function of a single-side-coupled microring resonator can be expressed as follows [6]:

$$T(\omega) = \frac{r - a\exp(i\phi)}{1 - ra\exp(i\phi)} \tag{1}$$

where r is the transmission coefficient, which is related to the coupling coefficient from the waveguide to the ring t as $r = \sqrt{1-t^2}$. $a = e^{-\frac{\alpha}{2}L}$ is the single pass attenuation in the ring, where L and α are the length of the ring and the linear loss, respectively. $\phi = kL$ is the linear phase shift of the ring, $k = \frac{n_{\mathrm{eff}}\omega}{c}$ is the propagation constant where n_{eff}, ω, and c are the effective refractive index, angular frequency, and the speed of light, respectively. Therefore, the group delay of the ring resonator can be expressed as [13], (2) as shown at the bottom of the page, where n_g is the group refractive index. Equation (2) reveals that the group delay achieves its maximum in the resonance wavelength and is reduced when detuned from the resonance.

When a pump light with a power of P_A is injected to the microring resonator, the absorbed energy is eventually converted to the thermal energy and leads to a temperature shift ΔT [10]

$$\frac{d\Delta T}{dt} + \frac{\Delta T}{\tau_\theta} = -\frac{P_A}{\rho C V} \tag{3}$$

where τ_θ of ~1 μs [10] is the thermal dissipation time of the crystalline silicon based on the experimental result in [11], the tuning speed of the delay line is limited by this thermal dissipation time on the order of microseconds. $\rho = 2.3 \times 10^{-3}$ kg/cm^3 is the density of the silicon, $C = 705$ J/(kg·K) is the thermal capacity, and V is the volume of the microring. The refractive index changes with the temperature as $\Delta n_\theta = k_\theta \Delta T$, where $k_\theta = 1.86 \times 10^{-4}$ K^{-1}. The change of the refractive index red shifts the resonance. As the thermooptic coefficient is very large in silicon, this thermal nonlinear effect has a low-power threshold. By using this method, the group delay of the signal can be changed by controlling the pump power with a low value.

B. Experimental Setup

The experiment setup is depicted in Fig. 3. The pump and the probe signal sit at two adjacent resonances in the vicinity of 1550 nm. A Mach–Zehnder modulator (MZM) is driven by an electrical PRBS signal of $2^7 - 1$ pattern length. We used the

$$T_D = \frac{(1-r^2)a^2}{1 - 2ra\cos(\phi)\frac{(1+a^2)}{2} + r^2a^2 + (\sin^2(\phi)(1-a^2)^2)r^2 - (1-a^2)} \frac{n_g L}{c} \tag{2}$$

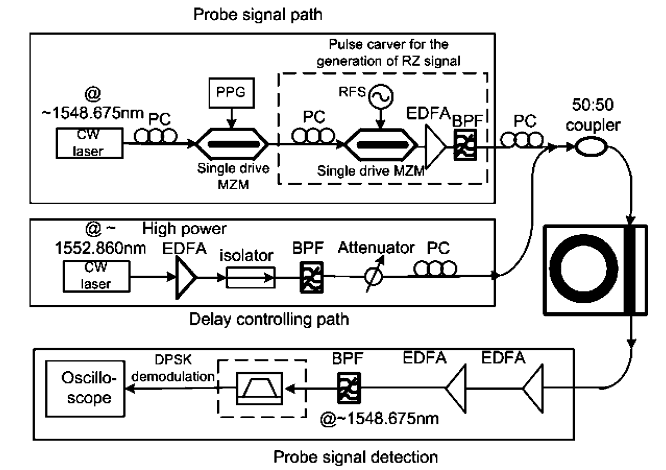

Fig. 3. Experimental setup of the optically tunable group delay using a single microring resonator. CW: Continuous wave; PC: Polarization controller; PPG: Pulse pattern generator; RFS: Radio frequency synthesizer; EDFA: Erbium-doped fiber amplifier; BPF: Bandpass filter.

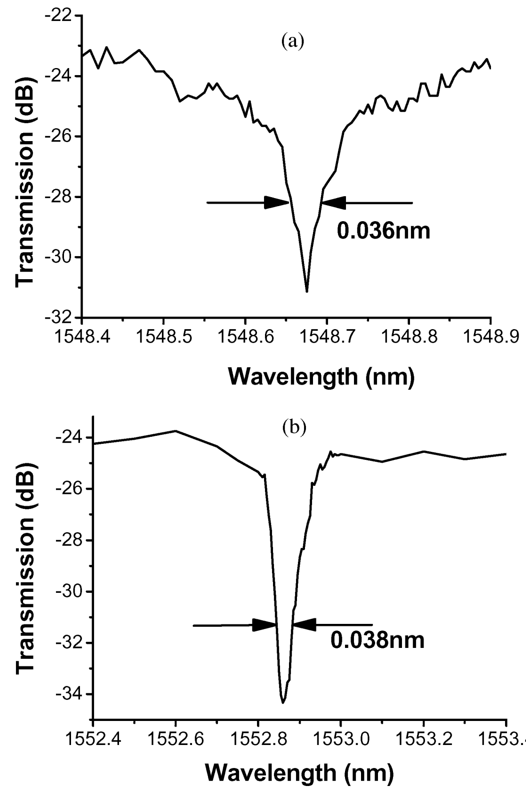

Fig. 4. Spectra of the resonances at (a) 1548.675 nm and (b) 1552.860 nm, respectively.

$2^7 - 1$ PRBS to facilitate the measurements of the delay, and experimental result shows that there is little difference if a longer pattern length is used. This MZM is biased at quadrature and null points of the transmission curve for generating NRZ and DPSK signals, respectively. The RZ signal is obtained by cascading a pulse carver through driving a second MZM using a sinusoidal signal with the same frequency as the data rate; hence, the duty cycle of the RZ signal is 50%. The pump light is amplified by a high-power erbium-doped fiber amplifier (EDFA) followed by an attenuator to adjust the pump power. Both the pump light and the probe signals are coupled through a 3 dB coupler to the microring resonator by the vertical coupling system. The output signal of the microring resonator is amplified using two cascaded EDFAs, and the probe signal is separated from the pump wave using a bandpass filter and fed to an oscilloscope to record the waveforms. When the probe signal is in DPSK format, we use a Mach–Zehnder delay interferometer (MZDI) to demodulate the DPSK signal. As the gold grating coupler is polarization-dependent, two polarization controllers are inserted before the coupler to make sure the input pump and probe lights are in the TE mode.

IV. Experimental Results

In this section, we experimentally examine the dependence of the delay on the pump power. Three typical modulation formats—NRZ, RZ, and DPSK signals are used. The spectral response of the microring resonator is shown in Section IV-A, the experimental results on the three modulation formats are presented in Sections IV-B–IV-D, and Sections IV-E and IV-F provide the summary of the observations and discussions.

A. Spectral Response of the Microring Resonator

To measure the spectral response of the microring resonator, we sweep the tunable laser with a minimum step of 0.005 nm. The measured spectra of the two resonances are shown in Fig. 4(a) and (b). The two resonance wavelengths are 1548.675 nm and 1552.860 nm, respectively. The resonance at 1548.675 nm has an 8 dB notch and the one at 1552.860 nm shows a 10 dB notch. The free spectral range (FSR) of the microring resonator is ∼4.18 nm. The 3 dB bandwidth is ∼0.036 nm for the resonance at 1548.675 nm and ∼0.038 nm for the resonance at 1552.860 nm. We set the pump wavelength at the right side of the resonance at 1552.860 nm to ensure that more power can be coupled into the resonator when the pump increases, since the thermal nonlinear effect detunes the resonance closer to the pump in this case. The signal wavelength is close to the resonance at 1548.675 nm.

B. Tunable Delay of the NRZ PRBS Data

We measured the delay performance of the NRZ PRBS signal at bit rates of 1 Gb/s, 5 Gb/s and 10 Gb/s, respectively. The power of the probe signal is fixed to ∼−7 dBm at the end of the input fiber in the experiment so that the power of the probe signal is sufficiently low to avoid heat generation. To verify the red-shift effect, we set the wavelength of the NRZ signal at the center and right of the resonance, respectively, and then increase the pump power. From Fig. 5(a), we find that the delay decreases monotonously with the increase of the pump power when the NRZ signal is initially at the center of the resonance; while in Fig. 6(a), the delay undergoes a peak when the NRZ signal is initially at the right of the resonance, which proves that the NRZ signal is tuned from the right side of the resonance to the center of the resonance. Further increasing the pump power shifts the NRZ signal to the left side of the resonance, corresponding to

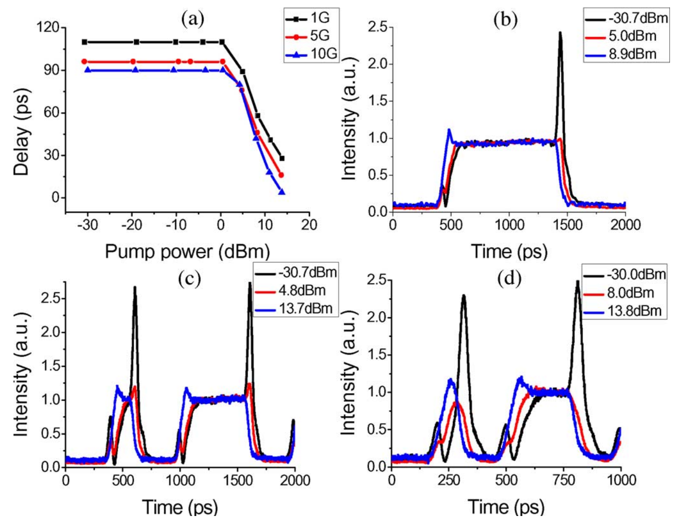

Fig. 5. (a) Delay versus pump power from the input fiber when the NRZ signal is initially at the center of the resonance. Waveforms of the delayed NRZ signals at (b) 1 Gb/s; (c) 5 Gb/s; (d) 10 Gb/s.

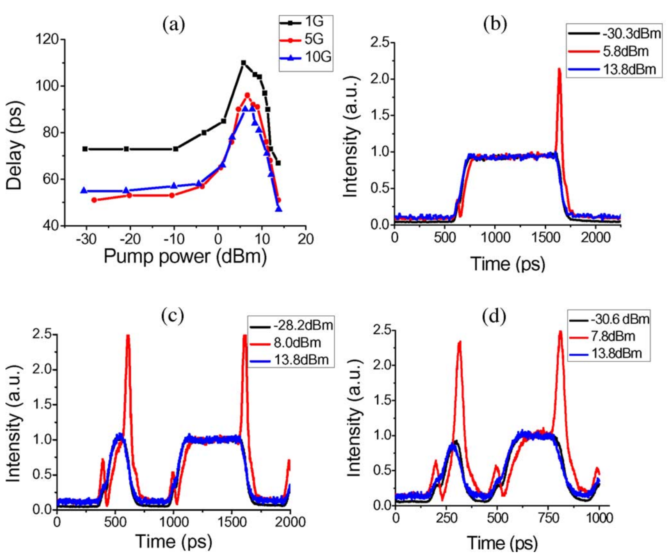

Fig. 6. (a) Delay versus pump power from the input fiber when the NRZ signal is initially at the right of the resonance. Waveforms of the delayed NRZ signals at (b) 1 Gb/s; (c) 5 Gb/s; (d) 10 Gb/s.

the red shift of the resonance. The NRZ signals at different data rates have nearly the same delay variations. The maximum delay for the 1-Gb/s, the 5-Gb/s and the 10-Gb/s NRZ signals are $\sim$110 ps, $\sim$100 ps and $\sim$90 ps, respectively. The threshold of the pump power is $\sim$ 0 dBm and a 15-dBm pump power from the input fiber ($\sim$5 dBm into the microring resonator) tunes the signal delay from $\sim$90 to $\sim$0 ps, which is close to the delay difference between on-resonance and off-resonance states. Here we obtained the delay by comparing the positions of the rising edges of the recorded waveforms from the oscilloscope (Figs. 5 and 6), and all the delays in the experiment are referred to the case when the probe signal is completely off-resonance. The waveform is normalized by the flat top of the "1" level. The 1-Gb/s NRZ data maintains its waveform except that a large overshoot appearing at the falling edge of the pulse at the

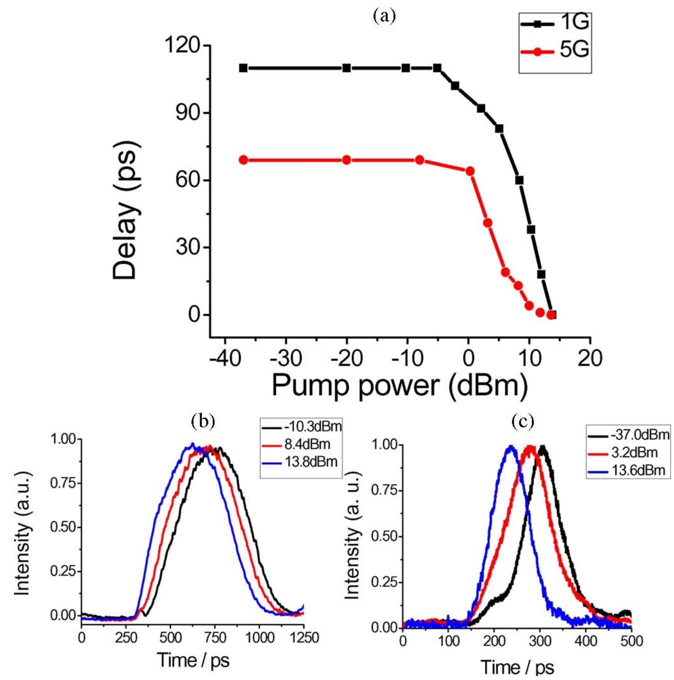

Fig. 7. (a) Delay of the 1 and 5 Gb/s RZ signals versus pump power from the input fiber. Waveforms of the delayed RZ signals at the data rate of (b) 1 Gb/s and (c) 5 Gb/s.

resonance wavelength; for the 5 Gb/s signal, there appear certain distortions. A large distortion can be observed for the 10 Gb/s signal at the resonance wavelength.

There are two factors contributing to the overshooting: 1) there are rapid changes of light intensity at the edges of the NRZ pulses that contain most of the high-frequency components. The notch filter preserves high-frequency components relative to the carrier frequency; thus, the edges of the pulses are expected to show higher transmission through the filter and 2) it has been known that the group velocity dispersion at the resonance is zero [14], and the third-order dispersion plays an important role; therefore, the filtered pulse is no longer symmetric showing an oscillatory structure near one of its edges depending on the sign of the third-order dispersion [15], [16]. For the silicon notch filter, the overshoots are seen at the falling edges of the pulses in the experiment. The overshoots observed in the experiment are also confirmed in [13].

C. Tunable Delay of the RZ PRBS Data

We also measured the delay performance for the RZ Gaussian-like pulse at data rates of 1 and 5 Gb/s. We obtained the delays by comparing the peak positions of the recorded pulse after normalizations. The distortion for the 10-Gb/s RZ signal is too severe to identify the delay. Fig. 7(a) shows the delay of the 1-Gb/s and the 5-Gb/s RZ signals as a function of the pump power when the RZ signals are initially at the center of the resonance. Fig. 7(b) and (c) shows the corresponding waveform at typical pump powers. We measured the bit-error-rate (BER) for the RZ signal when it is on-resonance and off-resonance, respectively [Fig. 8(a)]. The BER of the RZ signal on-resonance

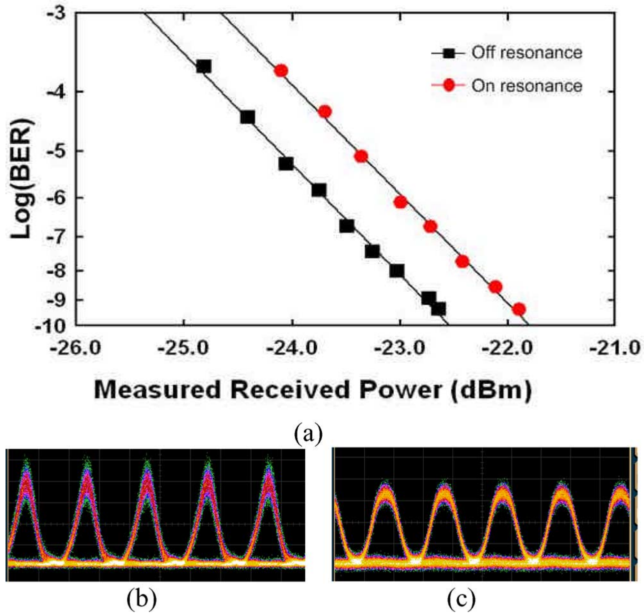

Fig. 8. (a) BER curves of the 5-Gb/s RZ signal when on-resonance and off-resonance; eye diagrams of the 5-Gb/s RZ signal for (b) on-resonance and (c) off-resonance with an OSNR of ∼20.5 dB and ∼22.5 dB, respectively.

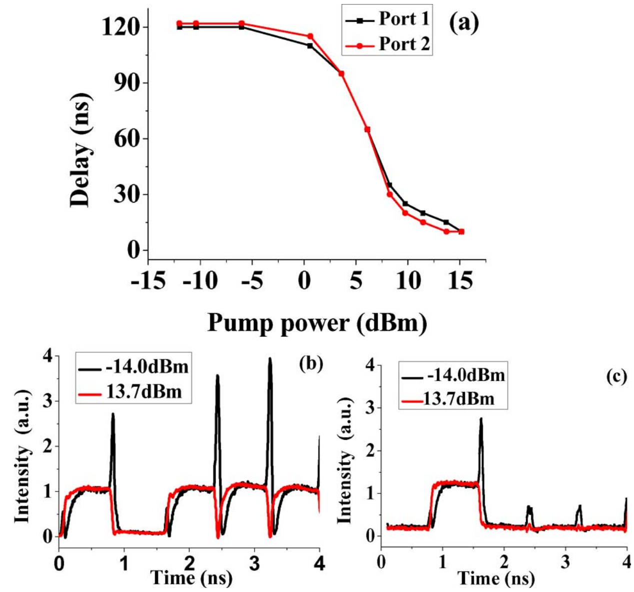

Fig. 9 (a) Delay of the demodulated 1.25-Gb/s DPSK signal versus the pump power from the input fiber; (b) and (c) Waveforms of the demodulated DPSK signal at two ports of the MZDI with a typical pump power of –14 dBm and 13.7 dBm, respectively.

shows a sensitivity penalty of ∼0.8 dB compared to the off-resonance case. Fig. 8(b) and (c) shows the eye diagrams for the 5-Gb/s RZ signal when it is on-resonance and off-resonance with an optical signal-to-noise ratio (OSNR) of ∼20.5 dB and ∼22.5 dB, respectively. The maximum delay is ∼110 ps for the 1 Gb/s signal and 70 ps for the 5 Gb/s signal; the threshold of the pump power is ∼0 dBm (∼−10 dBm into the microring resonator), which agrees with the results of the NRZ signals.

D. Tunable Delay of the DPSK PRBS Data

We take group delay of the demodulated signal to measure the delay of the DPSK signal, as in [17]. Fig. 9(a) shows the delay values of the demodulated DPSK signal at both the output ports of the MZDI as a function of the pump power, when the DPSK signal is initially at the center of the resonance. We find that there is little difference in delay between the signals at the two output ports of the MZDI. The data rate is set to 1.25 Gb/s to avoid strong filtering and demodulation effects from the microring resonator, thus maintaining the DPSK-signal quality before entering the MZDI. The constructive port of the MZDI outputs Duobinary signal, while the destructive port produces alter-mark inversion signal [17], [18]. Due to the limited resolution (0.07 nm) of the optical spectrum analyzer that cannot distinguish the optical spectra of the demodulated signals, we use “port 1” and “port 2” in Fig. 9(a) instead. Nevertheless the delay performances of the two demodulated signals are similar. The maximum delay for the DPSK signal is ∼120 ps with the signal on the resonance. Fig. 9(b) and (c) shows the typical waveforms of the demodulated DPSK signals at the two ports, respectively. Fig. 10 provides the eye diagrams of the delayed DPSK signals when on-resonance and off-resonance, respectively. Unlike the NRZ signal, there are large overshoots both at the rising and falling edge of the DPSK signal after passing through the ring when it is on-resonance.

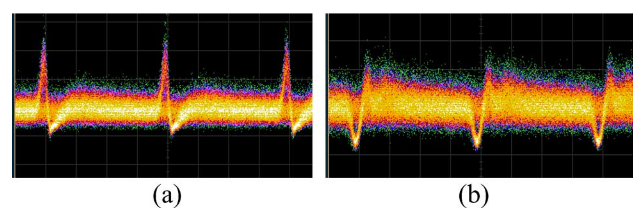

Fig. 10. Eye diagrams of the 1.25-Gb/s DPSK signals: (a) on-resonance, and (b) off-resonance.

E. Summary of the Observations

By comparing the experimental results of the three modulation formats, we find that: 1) the maximum group delays are nearly the same (∼120 ps) when the data rate is low; 2) the group delay begins to change at a pump power of ∼0 dBm at the input fiber for all the three modulation formats; 3) the needed pump power to detune the signal to about half of the maximum group delay is ∼6 dBm and the required pump power to shift the probe signal from on-resonance to off-resonance is ∼15 dBm at the input fiber; and 4) the three modulation formats have almost the identical group delays at the same data rate and similar dependence on the pump power. However, the RZ signal possesses better signal quality due to the smoother edges.

Therefore, this tunable delay line shows similar performances for the three modulation formats, which would be suitable for various applications employing different modulation formats.

F. Discussion

Based on the measured 3 dB bandwidth $\Delta\omega_{3\text{dB}}$, the transmission in the resonance ρ, and the FSR of the microring resonator $\Delta\omega_{\text{FSR}}$, we derive the coupling coefficient and the attenuation as [19]

$$t = \sqrt{\frac{\pi(1+\rho)\Delta\omega_{\text{FWHM}}}{\Delta\omega_{\text{FSR}}}} \tag{4a}$$

$$\alpha = \frac{\pi(1-\rho)\Delta\omega_{\text{FWHM}}}{\Delta\omega_{\text{FSR}} L}. \tag{4b}$$

From the measured resonance spectrum, we obtain the coupling coefficient $t = 0.2707$ and the attenuation $\alpha = 2.51$/cm. By substituting the results into the expression for the group delay, the group delay at the resonance wavelength is calculated to be 121 ps, which is very close to that measured in the experiment.

To predict the temperature change ΔT, we first derive the corresponding phase shift $\Delta\phi$ from the measured group delay using (2); then, the change of the refractive index Δn is related to the phase shift by $\Delta\phi = \frac{\Delta n \omega}{c} L$. Therefore $\Delta T = \frac{\Delta\phi c}{L\omega k_\theta}$. The estimated temperature change is ~0.4K when the group delay decreases to half of the maximum.

A single microring resonator is the building block for more complicated nanowaveguide based structures, which can support slow light operations. These structures consist of periodic spaced resonators with or without intercoupling, such as single-channel side-coupled integrated spaced sequence of resonators (SCISSOR), double-channel SCISSOR [14], and intercoupled resonators [20]. Our proposed optical tuning method might be used in these slow-light structures to tune the resonances of the microring resonators over a wide range.

V. Conclusion

We have experimentally demonstrated an optically tunable delay line based on the thermal nonlinear effect in the silicon microring resonator induced by the absorption of the pump light. The performance of this optically tunable delay line is examined using the NRZ, RZ, and DPSK PRBS signals. The required pump power to shift the probe signal from on-resonance to off-resonance is only ~5 dBm at the input of the microring.

References

[1] J. Bowers, E. Burmeister, and D. Blumenthal, "Optical buffering and switching for optical packet switching," presented at the Photon. Switching Conf., Crete, Greece, 2006, Paper O 16.1.

[2] R. Luijten, C. Minkenberg, R. Hemenway, M. Sauer, and R. Grzybowski, "Viable opto-elect HPC interconnect fabrics," in *Proc. ACM/IEEE SC2005 Supercomput. Conf.*, Seattle, WA, pp. 8–16.

[3] F. Xia, L. Sekaric, and Y. Vlasov, "Ultracompact optical buffers on a silicon chip," *Nat. Photon.*, vol. 1, pp. 65–71, Jan. 2007.

[4] B. Jalali and S. Fathpour, "Silicon photonics," *J. Lightw. Technol.*, vol. 24, no. 12, pp. 4600–4615, Dec. 2006.

[5] Y. Okawachi, M. Foster, J. Sharping, A. Gaeta, Q. Xu, and M. Lipson, "All-optical slow-light on a photonic chip," *Opt. Express*, vol. 14, no. 6, pp. 2317–2322, Mar. 2006.

[6] S. Blair and K. Zheng, "Intensity-tunable group delay using stimulated Raman scattering in silicon slow-light waveguides," *Opt. Express*, vol. 14, no. 3, pp. 1064–1069, Feb. 2006.

[7] B. Schmidt, Q. Xu, J. Shakya, S. Manipatruni, and M. Lipson, "Compact electro-optic modulator on silicon-on-insulator substrates using cavities with ultra-small modal volumes," *Opt. Express*, vol. 15, no. 6, pp. 3140–3148, Mar. 2007.

[8] F. Morichetti, A. Melloni, C. Canavesi, F. Persia, M. Martinelli, and M. Sorel, "Tunable slow-wave optical delay-lines," presented at the OSA Top. Meet. Slow Fast Light, Washington, DC, 2006, Paper MB2.

[9] D. Leuenberger, J. Yao, M. C. M. Lee, and M. C. Wu, "Experimental demonstration of MEMS-tunable slow light in silicon microdisk resonators," presented at the OSA Top. Meet. Slow Fast Light, Washington, DC, 2006, Paper TuC6.

[10] Q. Xu and M. Lipson, "Carrier-induced optical bistability in silicon ring resonators," *Opt. Lett.*, vol. 31, no. 3, pp. 341–343, Feb. 2006.

[11] V. R. Almeida and M. Lipson, "Optical bistability on a silicon chip," *Opt. Lett.*, vol. 29, no. 20, pp. 2387–2389, Oct. 2004.

[12] S. Scheerlinck, J. Schrauwen, F. Van Laere, D. Taillaert, D. Van Thourhout, and R. Baets, "Efficient, broadband and compact metal grating couplers for silicon-on-insulator waveguides," *Opt. Express*, vol. 15, no. 15, pp. 9639–9644, 2007.

[13] J. E. Heebner, "Nonlinear optical whispering gallery microresonators for photonics," Ph.D. dissertation [Online]. Available: http://www.optics.rochester.edu/workgroups/boyd/nonlinear.html

[14] J. Heebner and R. W. Boyd, "'Slow' and 'fast' light in resonator-coupled waveguides," *J. Mod. Opt.*, vol. 49, no. 14/15, pp. 2629–2636, 2002.

[15] Y. Wang, W. Hu, Y. Su, Z. Zheng, L. Leng, X. Tian, and Y. Jin, "Performance study of 40-Gb/s RZ signals through cascaded thin-film filters with large dispersion slope," *Opt. Express*, vol. 13, no. 6, pp. 2176–2181, Mar. 2005.

[16] G. P. Agrawal, *Nonlinear Fiber Optics*, 2nd ed. New York: Academic, 1995, ch. 3.

[17] B. Zhang, L. Yan, I. Fazal, L. Zhang, A. E. Willner, Z. Zhu, and D. J. Gauthier, "Slow light on Gbit/s differential-phase-shift-keying signals," *Opt. Express*, vol. 15, no. 4, pp. 1878–1883, Feb. 2007.

[18] L. Zhou, H. Chen, and A. W. Poon, "NRZ-to-PRZ format conversion using silicon second-order coupled-microring resonator-based notch filters," presented at the Conf. Lasers Electro-Opt. (CLEO) 2007, Baltimore, MD, Paper CThP4.

[19] C. Manolatou and M. Lipson, "All-optical silicon modulators based on carrier injection by two-photon absorption," *J. Lightw. Technol.*, vol. 24, no. 3, pp. 1433–1439, Mar. 2006.

[20] J. Scheuer, G. T. Paloczi, J. K. S. Poon, and A. Yariv, "Coupled resonator optical waveguides: Towards slowing and storing of light," *Opt. Photon. News*, vol. 16, no. 2, pp. 36–50, Feb. 2005.

Fangfei Liu (S'07) received the B.S. degree in electronic engineering in 2007 from the Department of Electronic Engineering, Shanghai Jiao Tong University, Shanghai, China, where she is currently a graduate student.

Her current research interests include advanced modulation formats for high-speed optical communication systems, nonlinear optics in waveguides and fibers, and optical signal processing.

Ms. Liu was the winner of the National Mathematical Modeling Contest in China in 2005.

Qiang Li (S'08) received the B.S. and M.S. degrees from Harbin Institute of Technology, Harbin, China, in 2005 and 2007, respectively. Currently, he is working toward the Doctoral degree at Shanghai Jiao Tong University, Shanghai, China.

His current research interests include slow light delay line and storage, and optical information processing in silicon waveguides.

Ziyang Zhang received the B.S. degree in optical engineering from Zhejiang University, Hangzhou, China, in 2003, and the M.S. degree in photonics from the Royal Institute of Technology (KTH), Stockholm, Sweden, in 2004. Currently, he is working toward the Ph.D. degree in the Department of Microelectronics and Applied Physics, KTH.

His current research interests include silicon-based photonic device simulation, fabrication, and characterization.

Min Qiu (M'99) received the B.Sc. and Ph.D. degrees from Zhejiang University, Hangzhou, China, in 1995 and 1999, respectively. He received the second Ph.D. degree in electromagnetic theory from the Royal Institute of Technology (KTH), Stockholm, Sweden, in 2001.

In 2001, he joined the Department of Microelectronics and Applied Physics, Royal Institute of Technology (KTH), where he is currently an Associate Professor. He also holds a Senior Researcher Fellowship from the Swedish Research Council, Stockholm, Sweden. He is the author or coauthor of more than 80 international refereed journal papers, and more than 60 conference contributions. His current research interests include optical metamaterials, photonic crystals, plasmonic optics, and integrated optical circuits.

Dr. Qiu is a member of the Optical Society of America and the European Optical Society. He was the recipient of the Individual Grant of Future Research Leader (INGVAR) from the Swedish Foundation for Strategic Research (SSF) in 2004.

Yikai Su (A'95–M'95–S'97–M'01–SM'07) received the B.S. degree from the Hefei University of Technology, Hefei, China, in 1991, the M.S. degree from the Beijing University of Aeronautics and Astronautics, Beijing, China, in 1994, and the Ph.D. degree in electronics engineering from Northwestern University, Evanston, IL, in 2001.

He was with Crawford Hill Laboratory of Bell Laboratories for 3 years before he joined the Shanghai Jiao Tong University, Shanghai, China, as a Full Professor in 2004. He became the Associate Department Chair of Electronic Engineering in 2006. He is the author or coauthor of more than 150 papes published in prestigious international journals and conferences, including 40 IEEE PHOTONICS TECHNOLOGY LETTERS papers, more than 20 invited conference presentations, and eight postdeadline papers. He is the holder of three U.S. patents with over 10 U.S. or Chinese patents pending. His current research interests include ultrahigh-speed transmission and modulation formats, optical signal processing, and enabling devices and modules.

Prof. Su is a member of the Optical Society of America. He serves as a Co-Chair of the Workshop on Optical Transmission and Equalization (WOTE) 2005, the ChinaCom 2007 Symposium, the IEEE/OSA AOE 2007 Slow Light Workshop, Asia Pacific Optical Communications (APOC) 2008 SC3, and a Technical Committee Member of the Opto-Electronics and Communications Conference (OECC) 2008, the Conference on Laser and Electro-Optics (CLEO) Pacific Rim (PR) 2007, the IEEE Lasers and Electro-Optics Society (LEOS) Summer Topical Meeting 2007 on ultrahigh-speed transmission, the IEEE Lasers and Electro-Optics Society (LEOS) 2005–2007, the BroadNets 2006, the Asia-Pacific Optical Communications (APOC) Conference 2005, and the International Conference on Optical Communications and Networks (ICOCN) 2004. He is a Guest Editor of the IEEE JOURNAL OF SELECTED TOPICS IN QUANTUM ELECTRONICS.